Influence of the parametrization of water optical properties on the modelled sea surface temperature in the Baltic Sea*

doi:10.5697/oc.55-1.053
OCEANOLOGIA, 55 (1), 2013.
pp. 53–76.

KEYWORDS
Baltic Sea
Sea surface temperature
Biological-physical interactions
Ocean models

Małgorzata Stramska[1,2,⋆]
Agata Zuzewicz[1,2]

[1] Institute of Oceanology,
Polish Academy of Sciences,
Powstańców Warszawy 55, Sopot 81–712, Poland;

e-mail: mstramska@iopan.gda.pl

⋆corresponding author

[2] Department of Earth Sciences,
Szczecin University,
Mickiewicza 16, Szczecin 70–383, Poland

Received 18 July 2012, revised 6 November 2012, accepted 26 November 2012.

Abstract

Treatment of light propagation in the water column requires further improvements in the biogeochemical models of the Baltic Sea. Regional models of the Baltic Sea usually assume a simple exponential vertical distribution of the total downward irradiance in the visible spectral range (PAR, photosynthetically available radiation). This is in spite of the fact that modelling studies for open ocean regions have stressed the importance of more detailed optical parameterization for the quality prediction of sea surface temperature and thermal structure of surface waters. In recent years extensive regional in situ bio-optical data sets have become available for the Baltic Sea, which can be used to develop a better understanding of the

* This work was supported by the SatBałtyk project funded by the European Union through the European Regional Development Fund (contract No. POIG.01.01.02-22-011/09 entitled 'The Satellite Monitoring of the Baltic Sea Environment').

feedbacks between optics and other processes simulated by the models. In this paper we compare four optical parameterizations used in numerical ocean models and their effects on modelled SSTs. This has been achieved using a one-dimensional ocean model coupled with the bio-optical models. Our results indicate that the differences between the various modelled SSTs using three optical parameterization schemes designed specifically for the Baltic Sea can give differences of up to 4°C in the modelled SSTs. This result warrants further research into the subject.

1. Introduction

The Baltic Sea is a shallow, brackish sea, which is of vital importance to the countries bordering it. During recent decades, the Baltic Sea has undergone considerable changes. Several studies have indicated that during the last 100 years, the temperature of the Baltic Sea has risen significantly more than has been observed in other surrounding seas (e.g. Siegel et al. 2006, Belkin 2009, Leppäranta & Myrberg 2009, Bradtke et al. 2010). The reasons for such a significant warming of the Baltic Sea remain unclear. At the same time eutrophication, stimulated by increased inputs of nutrients from agriculture, has become a major environmental issue in the Baltic Sea (HELCOM 2009). This is reflected in an increase in biomass and reduction in water transparency. Several modelling studies have investigated the eutrophication status of the Baltic Sea (Savchuk & Wulff 1999, 2007, Neumann et al. 2002, Neumann & Schernewski 2005, 2008), but the debate about the quantitative significance of different processes and the interactions involved is still ongoing. Trends in water temperature can have important implications for Baltic ecology and are most likely involved in feedback mechanisms that need to be closely investigated.

The main objective of this paper is to show that one of the aspects of the biogeochemical modelling of the Baltic Sea requiring further improvement is the treatment of light propagation in the water column. Regional models of the Baltic Sea usually employ simple irradiance penetration parameterizations and assume an exponential vertical distribution of the total downward irradiance in the visible spectral range (PAR, photosynthetically available radiation). This is in spite of the fact that recent model simulations for open oceanic regions have demonstrated that studies of mixed layer dynamics should include more detailed, spectrally-dependent, parameterizations of light attenuation (e.g. Zaneveld et al. 1981, Lewis et al. 1983, 1990, Simonot et al. 1988, Sathyendranath et al. 1991, Stramska & Dickey 1993). Differences in the parameterization of the penetrative irradiance component have been shown to affect the predicted sea surface temperature and the thermal structure of surface waters in the open ocean (e.g. Woods & Barkmann 1986, Stramska & Dickey 1993). Note that the attenuation of light in open ocean waters can often be approximated with sufficient

accuracy with the help of simplified Case 1 bio-optical relationships (e.g. Baker & Smith 1982, Morel 1988, Sathyendranath & Platt 1988, Mobley 1994, Kirk 2011). In coastal waters with high concentrations of coloured dissolved organic matter (CDOM) and/or mineral particles such as the Baltic Sea, these standard approaches developed for Case 1 waters should not be applied. However, there are no systematic studies evaluating the implications of differences in the parameterization of the vertical attenuation of light used in numerical models of the Baltic Sea.

In order to demonstrate that such differences can lead to significant discrepancies in simulated sea surface temperature (SST), we carried out a quantitative comparison of four different approaches. In the first approach we used a regional bio-optical model recently developed specifically for the Baltic Sea by Woźniak et al. (2008). In this case the propagation of radiant energy in the water column depends on the spectral vertical attenuation coefficient ($K_d(\lambda)$), which is a regionally-derived function of wavelength and chlorophyll *a* concentration (Chl). That is to say, by means of relatively simple statistical relationships, the spectral vertical attenuation coefficient ($K_d(\lambda)$) accounts for the total attenuation of light due to variable concentrations of phytoplankton, coloured dissolved organic matter (CDOM) and other optically active water components. In the second approach we used the 'standard' parameterization of the vertical attenuation coefficient for PAR (K_{PAR}) estimated as a simple function of chlorophyll concentration (Chl), which is often used in Baltic Sea models. In the third approach we applied a similar parameterization of K_{PAR}, but we tested the open ocean version of the parameterization. The fourth approach was based on the relationship between K_{PAR} and the vertical attenuation coefficient for downwelling irradiance at 490 nm ($K_d(490)$). In this case $K_d(490)$ can be estimated from satellite ocean colour data, so remote sensing data can provide the input for simulating the vertical attenuation of PAR. These four approaches for assessing underwater light fields were incorporated into the one-dimensional version of the Princeton Ocean Model (POM), based on Mellor and Yamada's turbulent closure scheme (e.g. Mellor & Yamada 1982). The POM model is well suited for investigating the temporal variability of SST and the thermal structure of the mixed layer resulting from both physical and biological effects.

The issue of optical influences on water temperature in the Baltic Sea has been addressed before. One of the first attempts in this respect was made by Kahru et al. (1993), who discussed feedbacks of cyanobacterial blooms on SST. More recently, the influence of increasing water turbidity on SST in the Baltic Sea was investigated by Löptien & Meier (2011). The main difference between our study and that of Löptien & Meier (2011) is that we used

a more detailed approach to the parameterization of irradiance attenuation (spectral dependence) and a different parameterization of vertical turbulent mixing in the physical model. Thus, one of our aims was to quantitatively compare the results of model simulations with the new parameterization of underwater irradiance (i.e. DESAMBEM) with those used in the past in modelling studies of the Baltic Sea.

2. Methods

2.1. Mixed layer model

In our study we used the level 2 1/2 version of the Mellor-Yamada model known as the Princeton Ocean Model (POM, Mellor & Yamada 1974, 1982, Mellor & Durbin 1975, Blumberg & Mellor 1983, Mellor 2004). This model belongs to the class of differential models and enables one to compute vertical profiles of turbulent variables. The model was modified to include the time-dependent vertical distribution of solar radiation, as described in the next section. One of the characteristic features of the POM is the realistic, stability-dependent eddy diffusivity parameterization, allowing interaction between heating and turbulence structure. Only the basic attributes of the Mellor-Yamada model are summarized here, as more details will be found in the papers cited above. The POM model is based on the solution of mean thermodynamic and momentum equations as well as turbulence equations, with some assumptions for closing the system of equations. For a horizontally homogeneous ocean with no average vertical water movement, the equations of conservation of momentum and heat may be written as:

$$\frac{\partial U}{\partial t} - f(V - V_g = \frac{\partial}{\partial z}\left[(K_M + \nu_M)\frac{\partial U}{\partial z}\right],$$

$$\frac{\partial V}{\partial t} - f(U - U_g = \frac{\partial}{\partial z}\left[(K_M + \nu_M)\frac{\partial V}{\partial z}\right],$$

$$\frac{\partial T}{\partial t} = \frac{\partial}{\partial z}\left[(K_H + \nu_H)\frac{\partial T}{\partial z}\right] + \frac{1}{\rho_o c_p}\frac{\partial I}{\partial z}, \tag{1}$$

where t is the time, z the vertical coordinate, U and V the mean horizontal velocity components, T the mean water temperature, I the irradiance, f the Coriolis parameter, K_M and K_H the eddy coefficients for vertical turbulent diffusion, ν_M and ν_H the coefficients for molecular and background diffusion, ρ_o the water density and c_p the specific heat of water. For simplicity, the geostrophic current components U_g and V_g are taken to be

zero. The equation set (1) is closed using the following formulas for the eddy coefficients:

$$K_M = l\,q\,S_M,$$
$$K_H = l\,q\,S_H, \tag{2}$$

where l is the turbulent length scale, $q^2/2$ the turbulent kinetic energy, and S_M and S_H are stability functions dependent on the local Richardson number. The Richardson number is defined as the ratio of the negative turbulent buoyancy production to the shear production. It is important to note that the equation of heat conservation in our version of POM differs from that used by Mellor and Yamada, because the vertical gradient of net irradiance I is included. We shall describe this term in greater detail in section 2.4.

For the numerical calculations, equations (1) were transformed into finite difference equations. Because we were interested in surface waters, the vertical grid spacing was optimized to obtain a higher vertical resolution near the surface. The distance between the computational grid points increased with depth according to a geometrical progression. The interval was ∼1 m at the surface and about 1.5 m at the deepest level, and there were 100 levels down to a depth of 123.73 m. The time step was set to 10 minutes.

2.2. Atmospheric forcing

Meteorological data from the NOAA-CIRES Climate Diagnostics Center NCEP/NCAR (National Center for Environmental Prediction and National Center for Atmospheric Research) Reanalysis 2 were used to parameterize the atmospheric forcing for the mixed layer model. The Reanalysis Project employs a state-of-the-art analysis/forecast system to assimilate global meteorological data from various available sources from 1948 to the present. In particular, the 6-hour average of zonal and meridional wind stress components, the latent, net long-wave and sensible heat flux estimates were used to establish surface boundary conditions for the model. In the model runs, the net heat loss, calculated as the sum of the latent, net long-wave and sensible heat fluxes, was applied at the sea surface. In addition, the short-wave radiation flux was assumed to penetrate into the water column and to act as the internal heat source (see next section and equation (1)). Note that for simplicity our version of the model assumed a null salinity flux at the ocean surface, i.e. the model did not account for changes in the water salinity due to sea ice processes, evaporation and precipitation. The latent heat of evaporation was included in the calculations of the net heat flux. We used NCEP data from 1998–2007 for the location on the open Baltic Sea

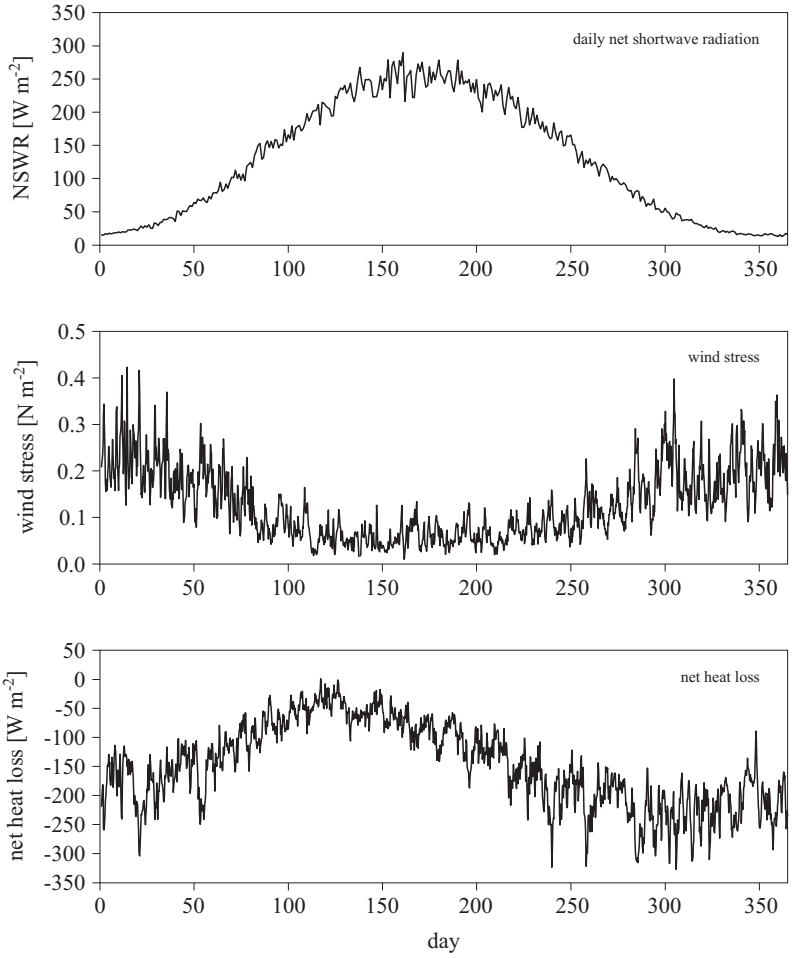

Figure 1. Annual 10-year averaged time series of (a) daily net shortwave radiation (NSWR), (b) wind stress magnitude, and (c) net heat loss, used as model input

(56.19°N, 18.75°E). Based on these data we calculated the 10-year averaged heat flux and wind stress time series, which were used as surface boundary conditions for all our model runs (Figure 1).

2.3. Initial conditions

The initial profiles of water temperature and salinity, which were used to start the calculations, were assumed to be the same for all our model simulations. These profiles were approximated on the basis of in situ data for station BY10 for January 2006, obtained from the Swedish National Marine Data Archive (SMHI, data available at produkter.smhi.se/pshark). The geographical position of station BY10 is 56°38.0′N and 19°35.0′E.

2.4. Bio-optical parameterizations

An important feature of our model is the detailed parameterization of the solar irradiance that penetrates into the water column. The vertical profiles of irradiance were calculated as follows. First, we obtained from the NCEP project the daily net short-wave radiation flux data just above the water surface for the location on the Baltic Sea (56.19°N, 18.75°E) and calculated the 10-year averaged time series of the daily net shortwave radiation flux. Using these data and the information on the average spectral composition of solar irradiance (e.g. Bird et al. 1983, Bird 1984) we calculated the radiative energy in specified spectral bands. A bandwidth of 10 nm for the visible light and broader bandwidths outside that spectral region were used. The derived spectral distribution of surface irradiance compares well with empirical results of other authors; that is, about 50% of the solar radiation is composed of visible light (Kishino et al. 1986, Smith & Baker 1986). In the next step, we calculated vertical profiles of the spectral downwelling irradiance beneath the water surface, assuming that about 94% of the radiative energy penetrates the surface and that the transmittance is wavelength-independent (Payne 1972, Smith & Baker 1986, Mobley 1994). We also assumed that there are two distinct fates of the solar radiative energy beneath the sea surface. First, we assumed that the radiant energy outside the visible region is attenuated by water molecules only, and that the effects of phytoplankton and other optically active water components can be neglected as a first approximation. The irradiance profiles in these spectral regions were calculated using the data compiled by Smith & Baker (1981) and Palmer & Williams (1974). According to these calculations, about half of the solar shortwave energy that is transferred across the water surface is absorbed in the top 1 m of the water column. The other half, the radiant energy from the visible spectral range, penetrates deeper into the water and its fate depends strongly on the optical properties of the water.

In all our calculations we assumed for simplicity that the water column is optically homogeneous. To approximately evaluate the effects of differences in parameterization of light attenuation we made two sets of simulations.

Inputs for the first set of model simulations – constant optical properties

The first set of simulations allowed us to compare the results from different model runs assuming that the optical properties in the water column are constant in time. In this set of simulations we used four approaches. For all four approaches we carried out model simulations, assuming in each case that $\mathrm{Chl} = 0.1, 0.4, 1.0, 5.0$ and 10 mg m^{-3}.

In the first approach $K_d(\lambda)$ was calculated from known Chl using the equations from the DESAMBEM algorithm:

$$K_d(\lambda) = K_w(\lambda) + \mathrm{Chl}\{c_1(\lambda)\ \exp[-a_1(\lambda)Chl] + k_{d,i}(\lambda)\} + \Delta K(\lambda), \quad (3)$$

where $\Delta K(\lambda)$ is defined as

$$\Delta K(\lambda) = 0.068\ \exp[-0.014(\lambda - 550)] \quad (4)$$

(Woźniak et al. 2008).

The numerical values of parameters $a_1(\lambda)$, $c_1(\lambda)$, $k_{d,i}(\lambda)$ and the diffuse attenuation coefficient for pure water $K_w(\lambda)$ are the same as in Woźniak et al. (2008) and are given in Table 1 for completeness. After calculating the spectral downwelling irradiance at each water depth using $K_d(\lambda)$ from equation (3), PAR was estimated at each model water depth as the spectrally integrated irradiance in the visible spectral range.

In the second approach we used a simple formula to calculate K_{PAR} from known Chl:

$$K_{\mathrm{PAR}} = K_{w2} + K_c\,\mathrm{Chl}, \quad (5)$$

where K_{w2} stands for the constant background attenuation of PAR (due to the combined optical effects of pure water and background concentrations of dissolved coloured and suspended matter) and K_c is the chlorophyll-specific PAR attenuation. We used the following numerical values for the parameters in equation (5). In the ERGOM simulations, $K_{w2} = 0.18$ m^{-1} and $K_c = 0.02$ m^2 mg^{-1}. These simulations were meant to follow the parameterization used in the ERGOM Baltic Sea Ecosystem Model (Neumann et al. 2000, 2002, 2005, 2008). In the original paper Neumann et al. (2000) used a nitrogen-based formulation of $K_{cN} = 0.03$ m^2 mmol^{-1}, by analogy with the nitrogen-based model of Fasham et al. (1990). Those authors showed that, with some assumptions about the average chemical composition of organic matter, $K_{cN} = 0.03$ m^2 mmol^{-1} corresponds to the chlorophyll-specific $K_c = 0.02$ m^2 mg^{-1}. We therefore used this value of K_c in our calculations. A similar parameterization of K_{PAR} has also been used in the past in the Production and Destruction of Organic Matter Model (ProDemo) (Ołdakowski et al. 2005). In this case the authors assumed that $K_{\mathrm{PAR}} = 0.17 + 0.025\,\mathrm{Chl}$. This formula leads to values of K_{PAR} quite similar to those in our set of ERGOM simulations (the differences are less than a few per cent).

In the third approach, for the set of simulations based on the parameterization from the Biogeochemical Elemental Cycling (BEC) ocean model, (Moore et al. 2002a,b, Moore et al. 2004), we also used equation (5) but with the numerical values of $K_{w2} = 0.04$ m^{-1} and $K_c = 0.03$ m^2 mg^{-1}. The

Table 1. Values of the parameters used in equation (3) (from Woźniak et al. 2008)

λ [nm]	a_1 [m^3 mgChl^{-1}]	c_1 [m^2 mgChl^{-1}]	$k_{d,\,i}$ [m^2 mgChl^{-1}]	K_w [m^{-1}]
400	0.441	0.141	0.0675	0.0209
410	0.495	0.137	0.0643	0.0197
420	0.531	0.131	0.0626	0.0187
430	0.580	0.119	0.0610	0.0177
440	0.619	0.111	0.0609	0.0176
450	0.550	0.107	0.0569	0.0181
460	0.487	0.0950	0.0536	0.0189
470	0.500	0.0970	0.0479	0.0198
480	0.500	0.0780	0.0462	0.0205
490	0.509	0.0774	0.0427	0.0230
500	0.610	0.0672	0.0389	0.0276
510	0.594	0.0598	0.0363	0.0371
520	0.590	0.0610	0.0319	0.0473
530	0.693	0.0573	0.0288	0.0513
540	0.606	0.0506	0.0285	0.0567
550	0.514	0.0432	0.0274	0.0640
560	0.465	0.0425	0.0248	0.0720
570	0.384	0.0288	0.0240	0.0810
580	0.399	0.0230	0.0231	0.107
590	0.365	0.0180	0.0231	0.143
600	0.333	0.0171	0.0225	0.212
610	0.304	0.0159	0.0216	0.236
620	0.316	0.0150	0.0225	0.264
630	0.421	0.0183	0.0225	0.295
640	0.420	0.0216	0.0226	0.325
650	0.346	0.0164	0.0236	0.343
660	0.348	0.0141	0.0260	0.393
670	0.173	0.00939	0.0267	0.437
675	0.173	0.00436	0.0270	0.455
680	0.173	0	0.0258	0.478
690	0	0	0.0190	0.535
700	0	0	0.0125	0.626
710	0	0	0.0045	1.000
720	0	0	0.0014	1.360
730	0	0	0.00041	1.810
740	0	0	$7.1\ 10^{-5}$	2.393
750	0	0	$1.3\ 10^{-5}$	2.990

BEC model is currently being adapted to the Baltic Sea by members of our team. The numerical values in the original BEC model were set up for open ocean simulations, and we are not planning to use these values in our future standard Baltic Sea version of the BEC model. Nevertheless, we decided to apply the original values in the current model simulations in order to demonstrate that the models developed for case 1 waters can lead to significant discrepancies when compared with the Baltic Sea models.

Finally, in the fourth approach we assumed that $K_d(490)$ is known. This allowed us to estimate K_{PAR} using the relationship between $K_d(490)$ and K_{PAR} derived for the Baltic Sea by Pierson et al. (2008). We used the following linear relationship (Pierson et al. 2008):

$$K_{\mathrm{PAR}} = 0.6098 K_d(490) + 0.1134. \tag{6}$$

In these calculations values of $K_d(490)$ were estimated from assumed Chl using the DESAMBEM formula, given by equation (5).

To illustrate the differences between the four approaches listed above, Figure 2 presents the vertical profiles of underwater downwelling irradiance

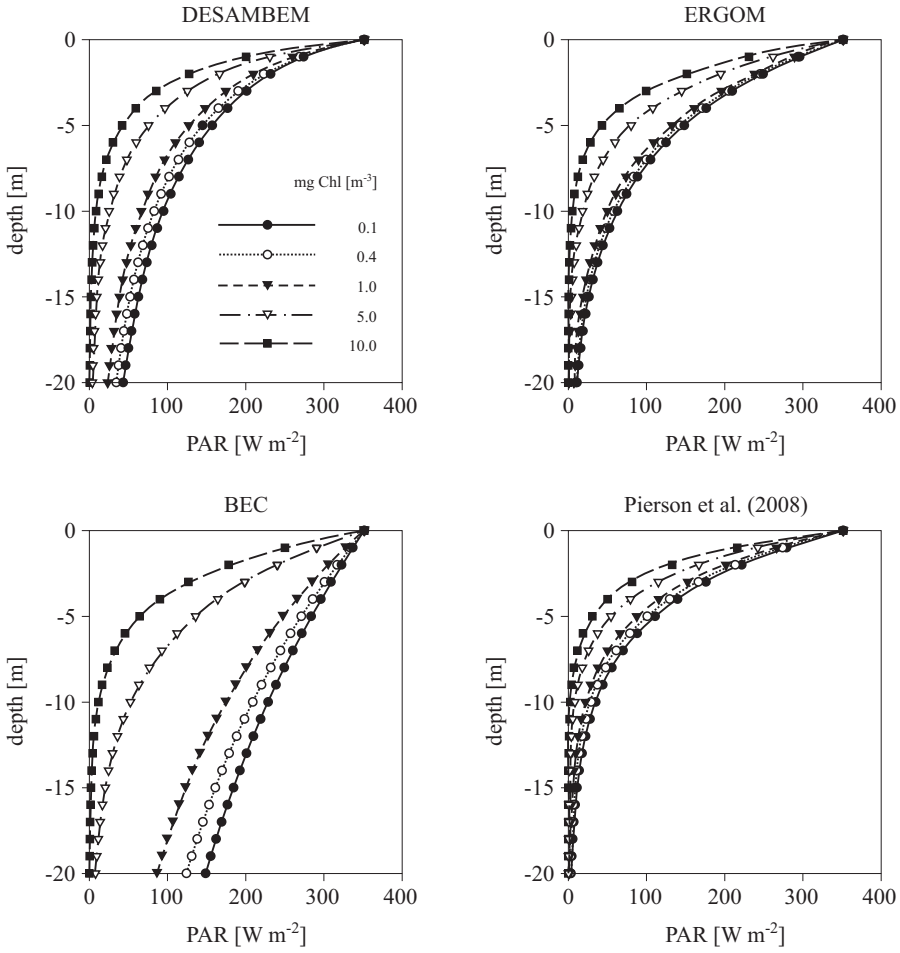

Figure 2. Vertical profiles of downwelling irradiance in the visible spectral range (PAR, W m^{-2}) estimated for a homogeneous water column with Chl = $0.1, 0.4, 1.0, 5.0$ and 10.0 mg m^{-3} using different parameterizations of the vertical diffuse attenuation coefficient. For explanations, see the text

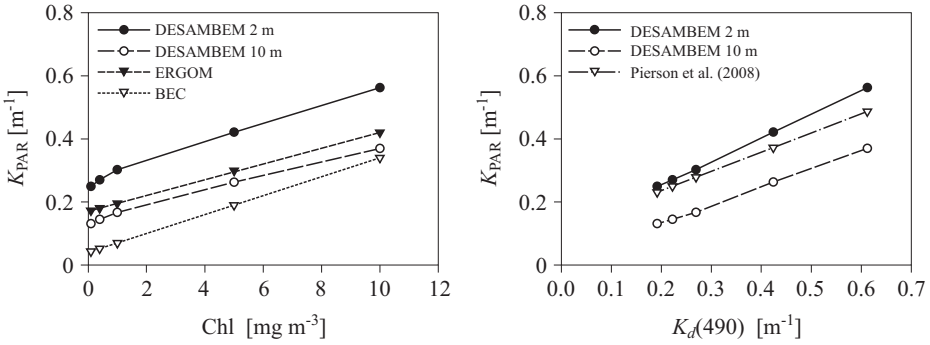

Figure 3. Relationships between the vertical diffuse attenuation coefficient K_{PAR} and Chl (left-hand panel) and K_{PAR} and $K_d(490)$ (right-hand panel) in different model simulations. For explanations, see the text

in the PAR spectral region calculated according to equations (3)–(6). In all cases PAR reaching the sea surface was assumed to be ∼340 W m^{-2}. It is clear from Figure 2 that there are significant differences in the simulated underwater light field in all four cases, with the highest values of PAR at depth for the BEC parameterization. This is to be expected, as BEC represents open ocean waters, which are much less turbid than Baltic Sea waters. In Figure 3, for comparison, we plotted K_{PAR} as a function of Chl (left-hand panel) and K_{PAR} as a function of $K_d(490)$ (right-hand panel) obtained using equations (3)–(6). Note that in each plot there are two lines for K_{PAR} derived from the DESAMBEM algorithm. This is because DESAMBEM is the only algorithm used in our simulations in which K_{PAR} is a function of water depth. This emerges from the fact that this algorithm uses the spectral dependence for the vertical diffuse light attenuation coefficient K_d. So in this case, the relationship between $K_d(490)$ and K_{PAR} was obtained by calculating $K_d(\lambda)$, estimating the spectral downwelling irradiance $E_d(\lambda z)$, and finally integrating $E_d(\lambda z)$ in the PAR spectral region at given water depths.

Note that in the real ocean, even in oligotrophic waters, the spectral composition of underwater radiation changes markedly with depth, due to the significant attenuation of light in the red wavebands by clear water. In the Baltic Sea light of shorter wavelengths is also significantly attenuated due to the presence of high concentrations of coloured dissolved organic matter (CDOM). Therefore, in real situations we would expect the PAR attenuation coefficient to be larger in the top few metres of the water column and to fall to lower values at greater depths (see Kirk (2011) for more detailed explanations). In our simulations, this feature of the underwater light field is only reproduced with the DESAMBEM algorithm.

Inputs for the second set of simulations – the annual cycle of the optical properties of water

Here we assumed that the optical properties of Baltic Sea waters are subject to an annual cycle. Such a cycle is observed in Baltic Sea waters as a consequence of the annual sequence of phytoplankton dynamics. The model simulations were carried out assuming two scenarios: 1) an annual cycle with 'low' Chl, and 2) an annual cycle with 'high' Chl. The time series of optical properties were obtained in two ways. First, we used the 1998–2011 time series of Chl recorded in the open sea (sites BY10, BY15 and BCSIII, data from the Swedish National Marine Data Archive, SMHI, available at produkter.smhi.se/pshark) to create the Chl time series. These Chl time series do not correspond to any specific year/location; rather, they should be regarded as 'synthetic data' that roughly reflect the range of variability of Chl in the Baltic Sea. The 'synthetic' time series of Chl used in our model simulations are plotted in Figure 4. These time series were used in turn to create the time series of $K_d(\lambda)$ using the DESAMBEM algorithm (eqs. (3) and (4)) and the K_{PAR} time series using eq. (5).

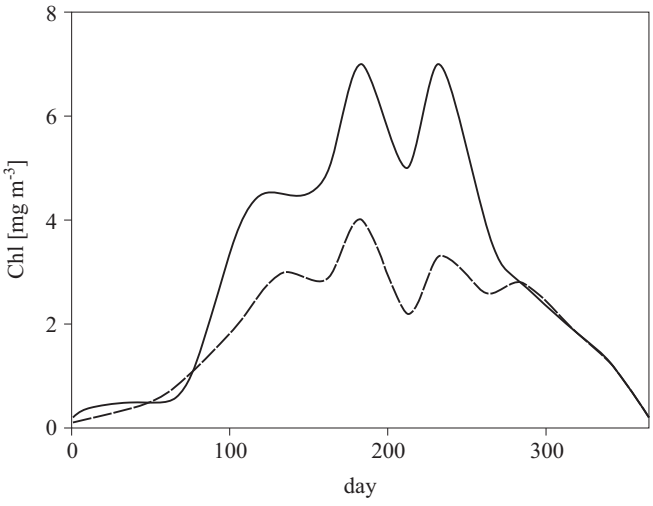

Figure 4. Time series of Chl used as input in some model simulations

Similarly, on the basis of satellite ocean colour data, we also created time series of $K_d(490)$. For this purpose we used the SeaWiFS and MODISA data available for the vicinity of stations BY10, BY15 and BCSIII (the same stations used to create the Chl time series). We used the NASA K_d_Lee(490) data product (McClain et al. 2004, Feldman & McClain 2012; data available at oceancolor.gsfc.nasa.gov), because for the Baltic Sea, it achieved the best performance of all the standard algorithms examined (Lee et al. 2005). We produced 'low' and 'high' $K_d(490)$ time series from all the available annual

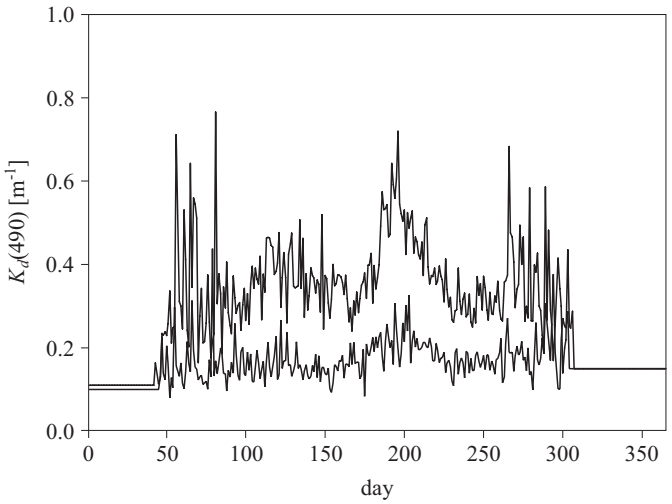

Figure 5. Time series of $K_d(490)$ used as input in some model simulations

satellite time series of K_d_Lee(490) data (Figure 5). These time series were then used to derive time series of $K_d(\lambda)$ using the DESAMBEM algorithm (equations (3) and (4)) and K_{PAR} time series using equations (6) (Pierson et al. 2008).

3. Results

3.1. First set of model simulations – constant optical properties

The results from the first set of model simulations are shown in Figures 6, 7, 8, and 9 for the parameterization of the vertical diffuse irradiance attenuation coefficient according to DESAMBEM, ERGOM, Pierson et al.

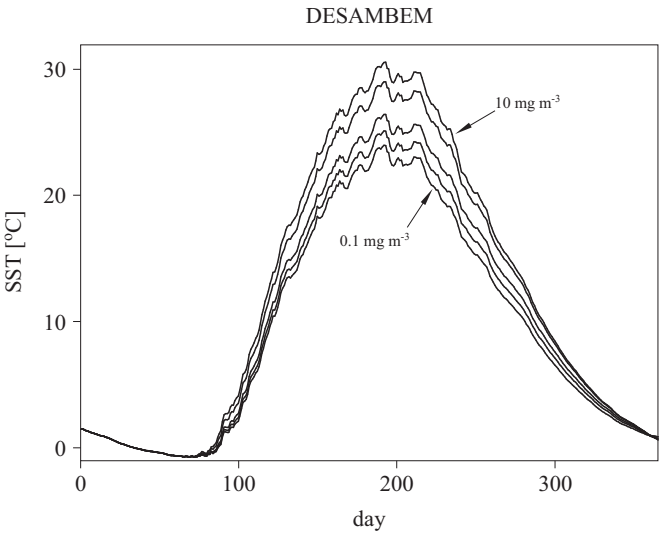

Figure 6. Time series of model-simulated SST using the DESAMBEM parameterization of $K_d(\lambda)$. The lines from bottom to top are for Chl = 0.1, 0.4, 1.0, 5.0, and 10.0 mg m^{-3} respectively

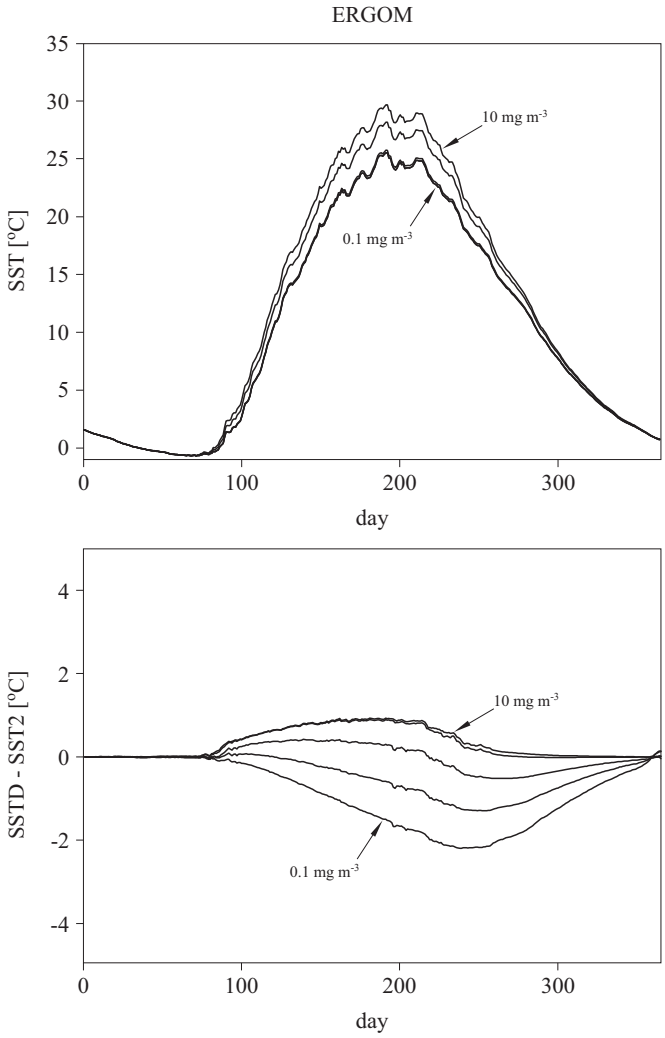

Figure 7. (Upper plot) Time series of model-simulated SST using the ERGOM parameterization of K_{PAR}. The lines from bottom to top are for $\mathrm{Chl} = 0.1, 0.4, 1.0, 5.0,$ and 10.0 mg m^{-3} respectively. (Lower plot) Time series of SST differences between the DESAMBEM SST (Figure 6) and the SST shown in the upper plot

(2008) and BEC, respectively. All the Figures show time series of model-simulated SSTs; in addition, the differences between SST obtained using the DESAMBEM parameterization (Figure 6) and the SST shown in the top panel of each Figure are also plotted in Figures 7, 8 and 9. Figures 6–9 show that in each case SST is the highest when Chl takes the greatest value. Comparison of all the simulations with the parameterizations from

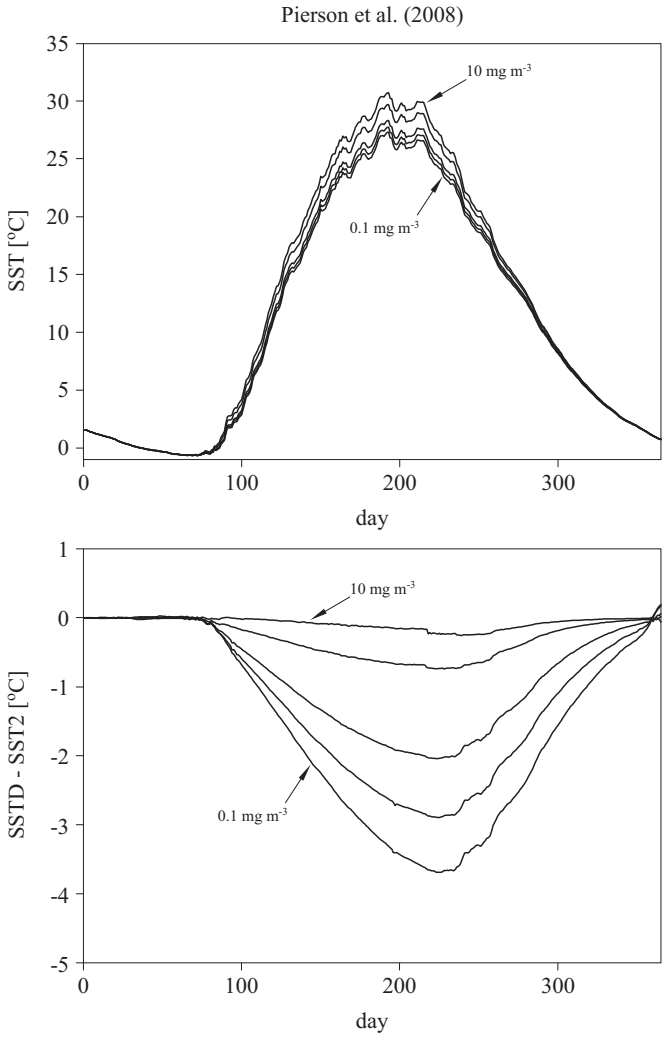

Figure 8. (Upper plot) Time series of model-simulated SST using the Pierson et al. (2008) parameterization of K_{PAR}. The lines from bottom to top are for Chl $= 0.1, 0.4, 1.0, 5.0$, and 10.0 mg m^{-3} respectively. (Lower plot) Time series of SST differences between the DESAMBEM SST (Figure 6) and the SST shown in the upper plot

various Baltic Sea studies (Figures 6, 7, and 8) shows that the DESAMBEM parameterization gives the broadest range of estimated annual maximum SSTs for model runs with Chl from 0.1 to 10 mg m^{-3}. We can also see that the parameterization according to Pierson et al. (2008) yields significantly higher values of SST than the DESAMBEM parameterization, especially for low Chl concentrations. For Chl $= 0.1$ mg m^{-3} the difference between

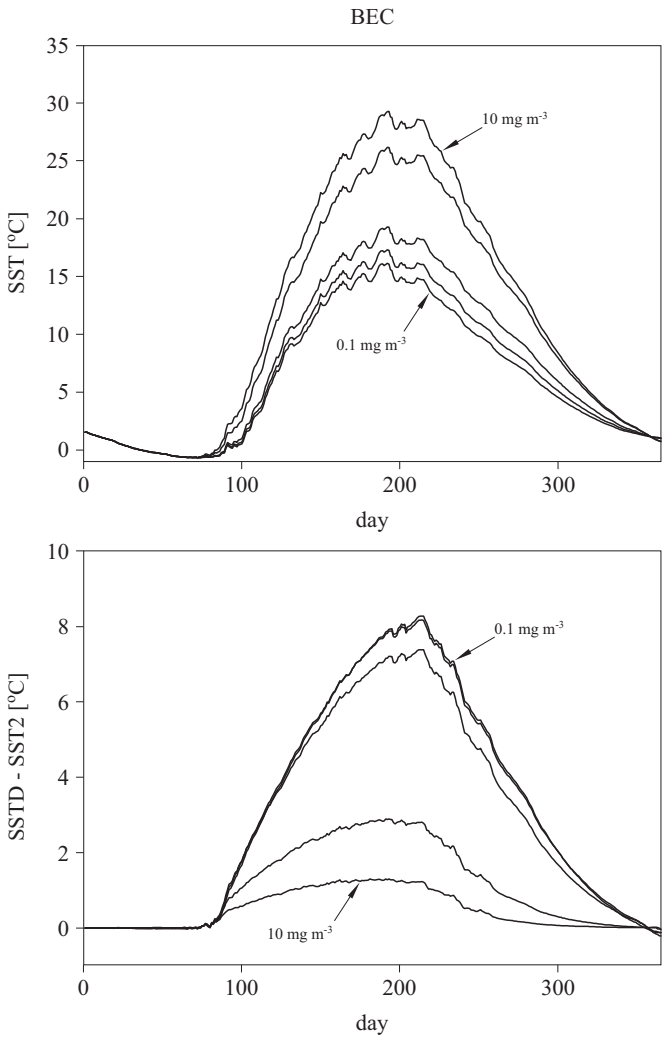

Figure 9. (Upper plot) Time series of model-simulated SST using the BEC (POP) parameterization of K_{PAR}. The lines from bottom to top are for Chl = $0.1, 0.4, 1.0, 5.0$, and 10.0 mg m^{-3} respectively. (Lower plot) Time series of SST differences between the DESAMBEM SST (Figure 6) and the SST shown in the upper plot

the DESAMBEM and the Pierson et al. (2008) parameterizations can lead to a difference in SST of about 4°C.

The BEC model (Figure 9) gives the widest range of all the modelled annual SST peak values. At low Chl concentrations BEC results yield the lowest SSTs of all our simulations. The maximum SST difference between the DESAMBEM and BEC simulations may be as much as 8°C. Here, we

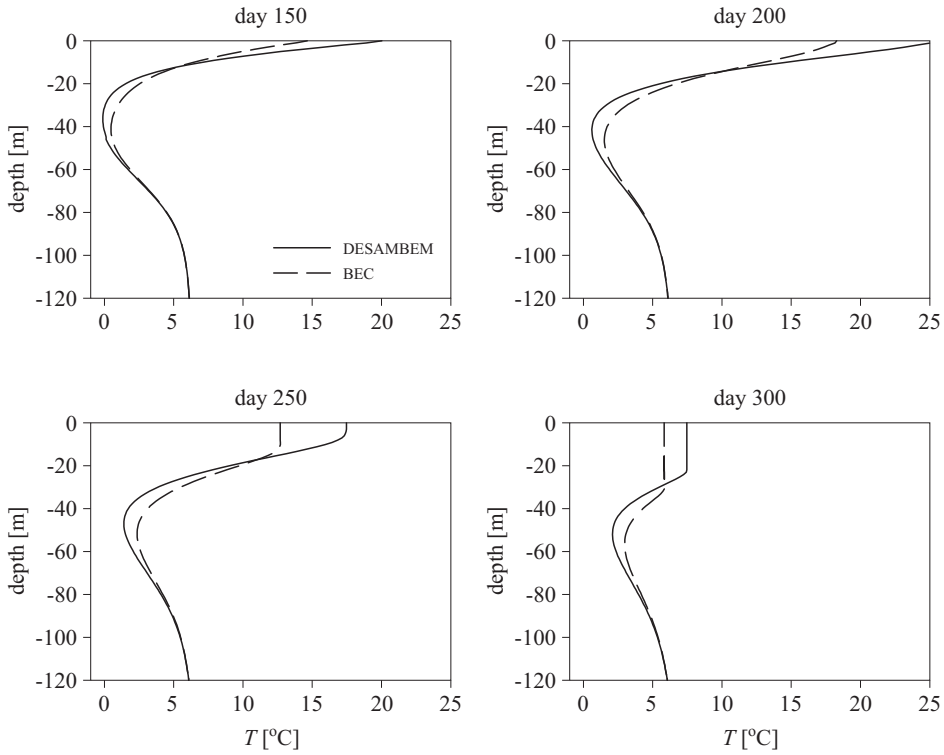

Figure 10. Vertical profiles of water temperature obtained from model simulations with the DESAMBEM and BEC (POP) optical parameterizations for Chl = 1 mg m^{-3}

recall that the BEC simulations apply the same K_{PAR} parameterization as is normally used for oceanic Case 1 waters. In such waters, when Chl concentrations are low, a significantly larger part of the radiant heating flux is transferred to greater depths than in the more turbid Baltic Sea waters. That is why surface waters warm up more slowly, especially in the BEC simulations for low Chl concentrations, than in the DESAMBEM simulations for the same Chl. In contrast, because more heat is transferred to a greater depth in the BEC than in the DESAMBEM simulations, at large depths the water will warm up more efficiently in the BEC model runs. This is shown in Figure 10, where the vertical profiles of water temperature are compared for the DESAMBEM and BEC results for the 150th, 200th, 250th and 300th days of the year. Although our main focus in this paper is SST, Figure 10 clearly shows that the differences in the K_d parameterizations can have a significant impact on the modelled water column temperature structure. This in turn may have important implications for the mixed layer depth (MLD) and modelled phytoplankton dynamics.

Second set of simulations – annual cycle of the optical properties of water

The results from our second set of simulations, i.e. the simulations with a prescribed annual cycle of water optical properties, are shown in Figures 11 and 12. They indicate that the difference between the DESAMBEM and ERGOM parameterizations of radiative heating for typical Baltic Sea conditions (Figure 11) can lead to a difference in SST of the order of 1°C in summer (with lower ERGOM SSTs). If the satellite $K_d(490)$ data product is used as input for model simulations, the modelled SST can differ by as much as 4°C, depending on whether the DESAMBEM or the Pierson et al. (2008) parameterization is used. Higher SSTs result from the Pierson et al. (2008) than from the DESAMBEM parameterization.

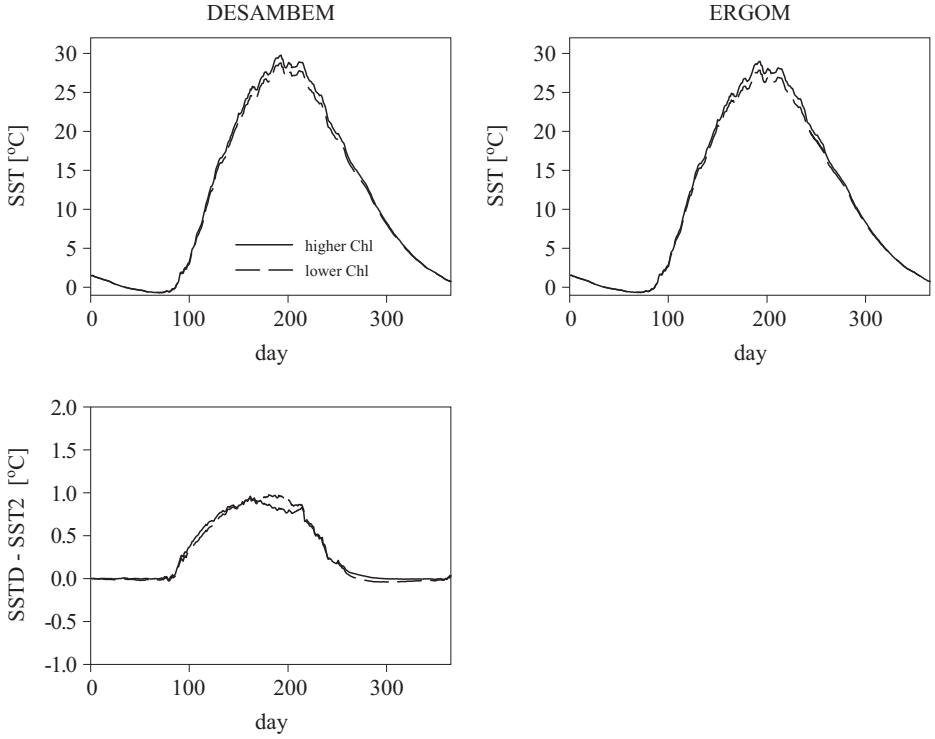

Figure 11. Comparison of model-simulated SST obtained with the DESAMBEM and ERGOM optical parameterizations when using time series of Chl concentration (shown in Figure 4) as model input

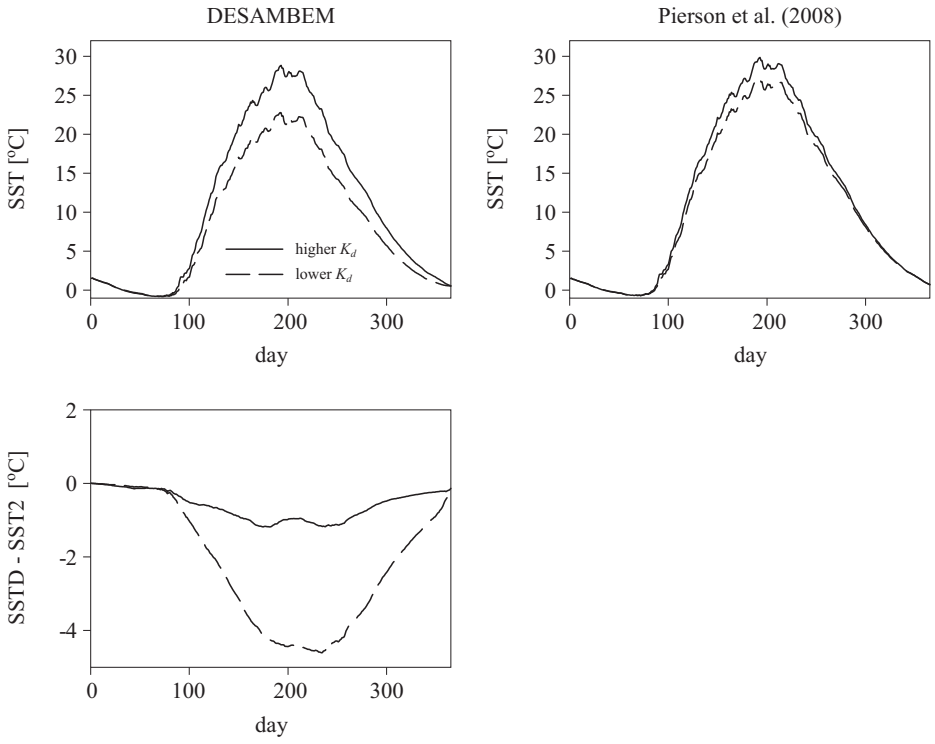

Figure 12. Comparison of model-simulated SST with the DESAMBEM and the Pierson et al. (2008) optical parameterizations when using time series of $K_d(490)$ (shown in Figure 5) as model input

4. Summary

It has been shown in the past that the optical state of oceanic waters affects the thermal structure of the upper ocean. This is because the local heating rate depends not only on the amount of solar radiation incident on the sea surface, but also on the vertical distribution of irradiance in the water column. The most important aim of this paper was to examine the effects of the differences in the optical parameterization schemes commonly used in numerical models of the Baltic Sea on modelled SST values. This was achieved using a one-dimensional model coupled with bio-optical models. Our results indicate that the choice of bio-optical parameterization method has significant effects on modelled SSTs and the vertical thermal stratification of the water column. We have shown that the differences between the various modelled SSTs using three parameterization schemes designed specifically for the Baltic Sea can result in to differences of up to 4°C in the modelled SSTs (the differences would be even greater if

parameterizations designed for open ocean waters were used). This result warrants further research into the subject.

At present we strongly believe that the DESAMBEM parameterization is the most reliable of the parameterizations examined in this paper, because this parameterization of $K_d(\lambda)$ is based on extensive in situ data sets collected in the Baltic Sea in recent years, which resolve the spectral dependence of $K_d(\lambda)$ (Darecki et al. 2008). Nevertheless, we shortly intend to undertake a meticulous validation of it with more sets of in situ data. A strong argument in favour of applying the DESAMBEM algorithm is that it uses the spectral parameterization of $K_d(\lambda)$; hence, it reflects the real features of the underwater light fields in the Baltic Sea more closely than the other parameterizations tested.

A number of benefits to our future modelling work will accrue from the coupling of an improved optical parameterization to the ecosystem model: (1) the subsurface light field will be more accurate, which is important for simulating light-sensitive biogeochemical processes such as photosynthesis and photo-oxidation, i.e. not just for estimating the warming up of waters discussed in this paper; (2) additional constraints on the model parameters may help to reduce uncertainties in the ecosystem model simulations; (3) better representation of the optics will make for easier comparison of the ecosystem model output with basic remotely-sensed ocean colour products. Furthermore, combining biogeochemical models with optics will pave the way for the future assimilation of ocean colour and in situ measured optical properties into the biogeochemical Baltic models.

Acknowledgements

The National Centers for Environmental Prediction and National Center for Atmospheric Research (NCEP/NCAR) Reanalysis Project meteorological data were provided by the NOAA-CIRES Climate Diagnostics Center. SeaWiFS and MODISA data (reprocessing 2010) were made available by NASAs Ocean Color Website (http://oceancolor.gsfc.nasa.gov/). We would also like to thank the Swedish National Marine Data Archive (SMHI) for access to Baltic Sea oceanographic data (produkter.smhi.se/pshark).

References

Baker K. S., Smith R. C., 1982, *Bio-optical classification and model of natural waters*, Limnol. Oceanogr., 27 (3), 500–509.

Bird R. E., 1984, *A simple, solar spectral model for direct-normal and diffuse horizontal irradiance*, Sol. Energy, 32 (4), 461–471, http://dx.doi.org/10.1016/0038-092X(84)90260-3.

Bird R. E., Hulstrom R. L., Lewis L. J., 1983, *Terrestrial solar spectral data sets*, Sol. Energy, 30 (6), 563–573, http://dx.doi.org/10.1016/0038-092X(83)90068-3.

Belkin I., 2009, *Rapid warming of large marine ecosystems*, Prog. Oceanogr., 81, 207–213.

Blumberg A. F., Mellor G. L., 1983, *Diagnostic and prognostic numerical circulation studies of the South California Bight*, J. Geophys. Res., 88 (8), 4579–4592, http://dx.doi.org/10.1029/JC088iC08p04579.

Bradtke K., Herman A., Urbański J. A., 2010, *Spatial and interannual variations of seasonal sea surface temperature patterns in the Baltic Sea*, Oceanologia, 52 (3), 345–362, http://dx.doi.org/10.5697/oc.52-3.345.

Darecki M., Ficek D., Krężel A., Ostrowska M., Majchrowski R., Woźniak S. B., Bradtke K., Dera J., Woźniak B., 2008, *Algorithms for the remote sensing of the Baltic ecosystem (DESAMBEM). Part 2: Empirical validation*, Oceanologia, 50 (4), 509–538.

Fasham M. J. R., Ducklow H. W., McKelvie S. M., 1990, *A nitrogen-based model of plankton dynamics in the oceanic mixed layer*, J. Mar. Res., 48 (3), 591–639.

Feldman G. C., McClain C. R., 2012, *Ocean Color Web. SeaWiFS and MODISA Reprocessing 2010*, N. Kuring & S. W. Bailey (eds.), NASA Goddard Space Flight Center, http://oceancolor.gsfc.nasa.gov/, (access date January 2012).

HELCOM 2009, *Eutrophication in the Baltic Sea – An integrated thematic assessment of the effects of nutrient enrichment and eutrophication in the Baltic Sea region*, Balt. Sea Environ. Proc. No. 115B, 148 pp.

Kahru M., Leppänen J. M., Rud O., 1993, *Cyanobacterial blooms cause heating of the sea surface*, Mar. Ecol.-Prog. Ser., 101, 1–7.

Kirk J. T. O., 2011, *Light and photosynthesis in aquatic ecosystems*, Cambridge Univ. Press, 3rd edn., Cambridge, 662 pp.

Kishino M., Okami N., Takahashi M., Ichimura S. E., 1986, *Light utilization efficiency and quantum yield of phytoplankton in a thermally stratified sea*, Limnol. Oceanogr., 31 (3), 557–566.

Lee Z.-P., Darecki M., Carder K. L., Davis C. O., Stramski D., Rhea W. J., 2005, *Diffuse attenuation coefficient of downwelling irradiance: An evaluation of remote sensing methods*, J. Geophys. Res., 110, C02017, http://dx.doi.org/10.1029/2004JC002573.

Leppäranta M., Myrberg K., 2009, *Physical oceanography of the Baltic Sea*, Springer, Berlin, [ISBN: 978-3-540-79702-9], 378 pp.

Lewis M. R., Carr M. E., Feldman G. C., Esaias W., McClain C., 1990, *Influence of penetrating solar radiation on the heat budget of the equatorial Pacific Ocean*, Nature, 347 (6293), 543–545, http://dx.doi.org/10.1038/347543a0.

Lewis M. R., Cullen J. J., Platt T., 1983, *Phytoplankton and thermal structure in the upper ocean: consequences of nonuniformity in the chlorophyll profile*, J. Geophys. Res., 88 (C4), 2565–2570, http://dx.doi.org/10.1029/JC088iC04p02565.

Löptien U., Meier H. E. M., 2011, *The influence of increasing water turbidity on the sea surface temperature in the Baltic Sea: A model sensitivity study*, J. Marine Syst., 88 (2), 323–331.

McClain C. R., Feldman G. C., Hooker S. B., 2004, *An overview of the SeaWiFS project and strategies for producing a climate research quality global ocean bio-optical time series*, Deep Sea Res. Pt. II, 51 (1–3), 5–42, http://dx.doi.org/10.1016/j.dsr2.2003.11.001.

Mellor G. L., 2004, *Users guide for a three – dimensional, primitive equation numerical ocean model*, available on the Princeton Ocean Model (POM) website, rev.2004, http://www.aos.princetion.edu/WWPUBLIC/htdocs.pom/.

Mellor G. L., Durbin P. A., 1975, *The structure and dynamics of the ocean surface mixed layer*, J. Phys. Oceanogr., 5 (4), 718–728, http://dx.doi.org/10.1175/1520-0485(1975)005<0718:TSADOT>2.0.CO;2.

Mellor G. L., Yamada T., 1974, *A hierarchy of turbulence closure models for planetary boundary layers*, J. Atmos. Sci., 31 (7), 1791–1806, http://dx.doi.org/10.1175/1520-0469(1974)031<1791:AHOTCM>2.0.CO;2.

Mellor G. L., Yamada T., 1982, *Development of a turbulence closure model for geophysical fluid problems*, Rev. Geophys. Space Phys., 20 (4), 851–857, http://dx.doi.org/10.1029/RG020i004p00851.

Mobley C. D., 1994, *Light and water: Radiative transfer in natural waters*, Acad. Press, New York, 592 pp.

Moore J. K., Doney S. C., Glover D. M., Fung I. Y., 2002a, *Iron cycling and nutrient limitation patterns in surface waters of the world ocean*, Deep Sea Res. Part II, 49 (1–3), 463–508, http://dx.doi.org/10.1016/S0967-0645(01)00109-6.

Moore J. K., Doney S. C., Kleypas J. C., Glover D. M., Fung I. Y., 2002b, *An intermediate complexity marine ecosystem model for the global domain*, Deep Sea Res. Part II, 49 (1–3), 403–462, http://dx.doi.org/10.1016/S0967-0645(01)00108-4.

Moore J. K., Doney S. C., Lindsay K., 2004, *Upper ocean ecosystem dynamics and iron cycling in a global three-dimensional model*, Global Biogeochem. Cy., 18 (4), GB4028, http://dx.doi.org/10.1029/JC093iC09p10749.

Morel A., 1988, *Optical modeling of the upper ocean in relation to its biogenous matter content (case 1 waters)*, J. Geophys. Res., 93 (C9), 10749–10768.

Neumann T., 2000, *Towards a 3D-ecosystem model of the Baltic Sea*, J. Marine Syst., 25 (3–4), 405–419, http://dx.doi.org/10.1016/S0924-7963(00)00030-0.

Neumann T., Fennel W., Kremp C., 2002, *Experimental simulations with an ecosystem model of the Baltic Sea: A nutrient load reduction experiment*, Global Biogeochem. Cy., 16, 1033, http://dx.doi.org/10.1029/2001GB001450.

Neumann T., Schernewski G., 2005, *An ecological model evaluation of two nutrient abatement strategies for the Baltic Sea*, J. Marine Syst., 56 (1–2), 195–206, http://dx.doi.org/10.1016/j.jmarsys.2004.10.002.

Neumann T., Schernewski G., 2008, *Eutrophication in the Baltic Sea and shifts in nitrogen fixation analyzed with a 3D ecosystem model*, J. Marine Syst., 74 (1–2), 592–602, http://dx.doi.org/10.1016/j.jmarsys.2008.05.003.

Ołdakowski B., Kowalewski M., Jędrasik J., Szymelfenig M., 2005, *Ecohydrodynamic model of the Baltic Sea. Part 1. Description of the ProDeMo model*, Oceanologia, 47 (4), 477–516.

Palmer K. F., Williams D., 1974, *Optical properties of water in the near infrared*, J. Opt. Soc. Am., 64 (8), 1107–l110, http://dx.doi.org/10.1364/JOSA.64.001107.

Payne R. E., 1972, *Albedo of the sea surface*, J. Atmos. Sci., 29 (5), 959–970, http://dx.doi.org/10.1175/1520-0469(1972)029<0959:AOTSS>2.0.CO;2.

Pierson D., Kratzer S., Strömbeck N., Hakànsson B., 2008, *Relationship between the attenuation of downwelling irradiance at 490 nm with the attenuation of PAR (400 nm – 700 nm) in the Baltic Sea*, Remote Sens. Environ., 112 (3), 668–680, http://dx.doi.org/10.1016/j.rse.2007.06.009.

Savchuk P. O., Wulff F., 1999, *Modeling regional and large-scale response of Baltic Sea ecosystems to nutrient load reductions*, Hydrobiologia, 393 (1), 35–43.

Savchuk P. O., Wulff F., 2007, *Modeling the Baltic Sea eutrophication in a decision support system*, AMBIO 36 (2), 141–148, http://dx.doi.org/10.1579/0044-7447(2007)36[141:MTBSEI]2.0.CO;2.

Sathyendranath S., Gouveia A. D., Shetye S. R., Ravindran P., Platt T., 1991, *Biological control of surface temperature in the Arabian Sea*, Nature, 349 (6304), 54–56, http://dx.doi.org/10.1038/349054a0.

Sathyendranath S., Platt T., 1988, *The spectral irradiance field at the surface and in the interior of the ocean: A model for applications in oceanography and remote sensing*, J. Geophys. Res., 93 (C8), 9270–9280, http://dx.doi.org/10.1029/JC093iC08p09270.

Siegel H., Gerth M., Tschersich G., 2006, *Sea surface temperature development of the Baltic Sea in the period 1990–2004*, Oceanologia, 48 (S), 119–131.

Simonot J.-Y., Dollinger E., Le Treut H., 1988, *Thermodynamic-biological-optical coupling in the oceanic mixed layer*, J. Geophys. Res., 93 (C7), 8193–8202, http://dx.doi.org/10.1029/JC093iC07p08193.

Smith R. C., Baker K. S., 1981, *Optical properties of the clearest natural waters (200–800 nm)*, Appl. Opt., 20 (2), 177–184, http://dx.doi.org/10.1364/AO.20.000177.

Smith R. C., Baker K. S., 1986, *Analysis of ocean optical data*, II. Proc. Sot. Photo-Optical Eng., 637, 95–107.

Stramska M., Dickey T., 1993, *Phytoplankton bloom and the vertical thermal structure of the upper ocean*, J. Mar. Res., 51 (4), 819–842.

Woods J. D., Barkmann W., 1986, *The response of the upper ocean to solar heating. I. The mixed layer*, Q. J. Roy. Meteor. Soc., 112 (471), 1–27, http://dx.doi.org/10.1002/qj.49711247102.

Woźniak B., Krężel A., Darecki M., Woźniak S. B., Majchrowski R., Ostrowska M., Kozłowski Ł., Ficek D., Olszewski J., Dera J., 2008, *Algorithms for the remote sensing of the Baltic ecosystem (DESAMBEM). Part 1: Mathematical apparatus*, Oceanologia, 50 (4), 451–508.

Zaneveld J. R., Kitchen J. C., Pak H., 1981, *The influence of optical water type on the heating rate of a constant depth mixed layer*, J. Geophys. Res., 86 (C7), 6426–6428, http://dx.doi.org/10.1029/JC086iC07p06426.